

Electromagnetic studies in the Eastern Mediterranean Region with Special Reference to Major Strike-slip Faults

Faults and fluids: an essential combination for (major) earthquakes?

Sabri Bülent Tank¹

bulent.tank@boun.edu.tr

¹*Boğaziçi University, Kandilli Obs. & E.R.I., İstanbul*



EMIW **XXV ELECTROMAGNETIC INDUCTION WORKSHOP**
2022
11-17 September 2022
Grand Hotel Ontur Çeşme-Turkey



Türkoğlu, Kahramanmaraş prefecture, PC: TRT



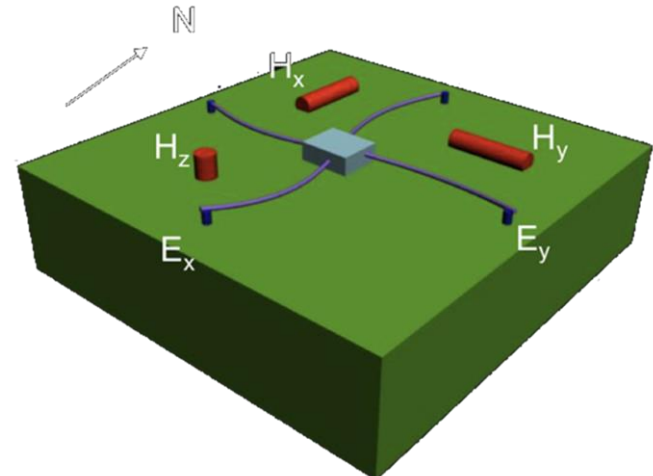
Tepehan, Hatay prefecture, PC: TRT



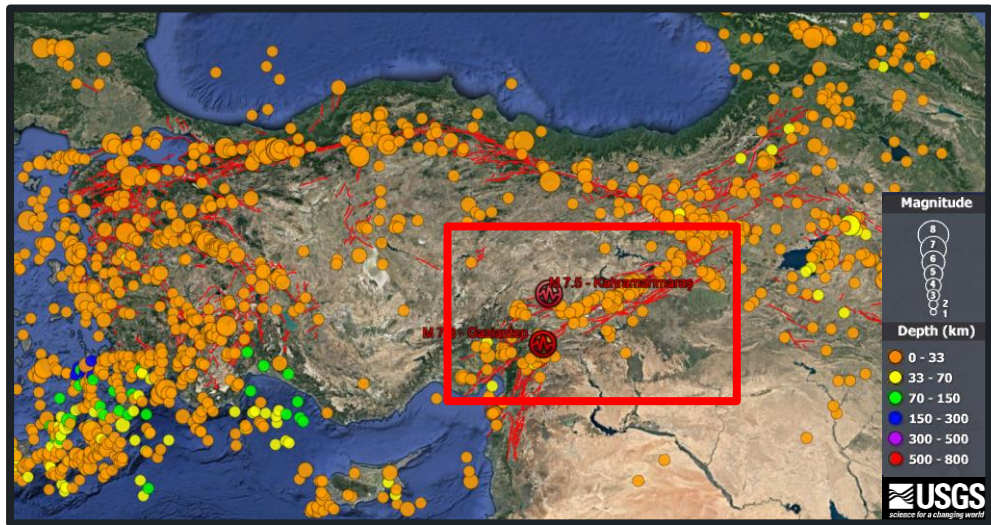


Outline

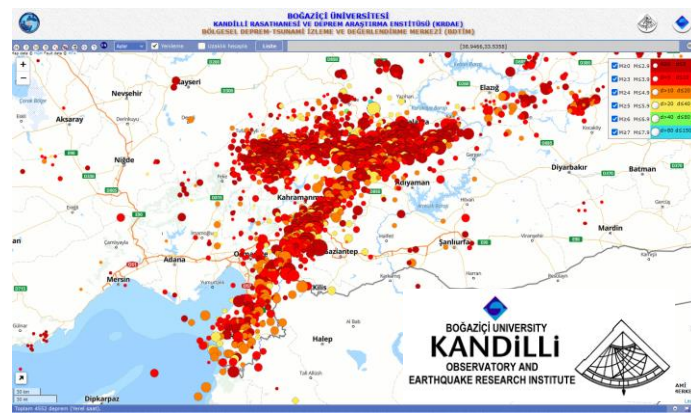
-
- Recent activity
 - 2023 Earthquakes
 - Coulomb stress maps
 - (I) Strike-slip (transform) faults
 - Fault zone architecture and Earthquakes
 - EM studies on (strike-slip) faults:
 - Theory
 - Global examples:
 - Alpine Fault, New Zealand
 - San Andreas Fault, California, the USA
 - Atotsugawa Fault, Central Honshu, Japan
 - AltynDagh Fault, W. China
 - Phayao Fault, N. Thailand
 - Bogd, Trans Altai, Tienshan faults, Mongolia
 - (II) Tectonics of the Study Area (Eastern Mediterranean)
 - (III) EM on the major strike-slip faults in the Eastern Mediterranean
 - A collage of transform faults
 - Dead Sea Transform Fault
 - East Anatolian Fault
 - North Anatolian Fault
 - (IV) Discussion
 - 2D vs 3D
 - Shallow structure
 - Deep structure
 - (V) Conclusion
 - Call for projects



2023 Earthquakes



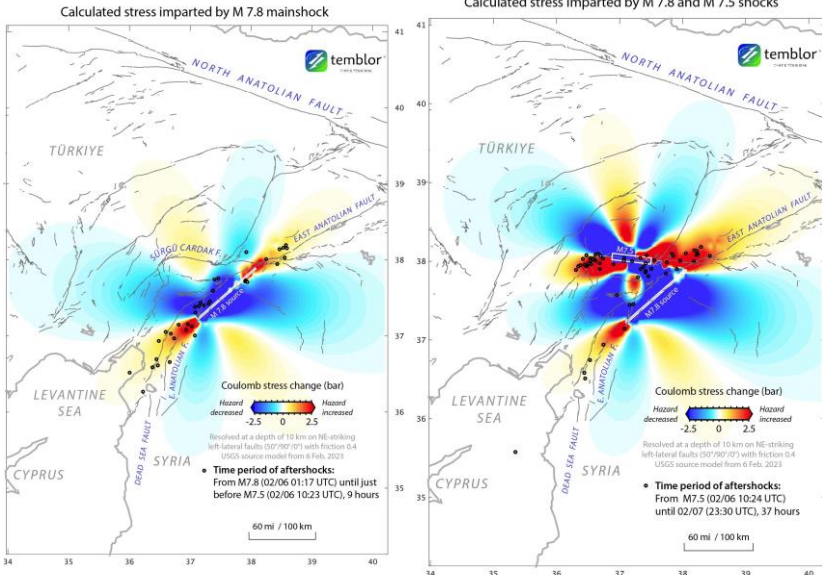
Earthquakes 1900 – 2023 (Source: USGS)



Distributions of aftershocks (06.02.2023 – 13.02.2023)

Kandilli Observatory And Earthquake Research Institute, Boğaziçi University. (1971). Bogazici University Kandilli Observatory And Earthquake Research Institute [Data set]. International Federation of Digital Seismograph Networks. <https://doi.org/10.7914/SN/KO>

Coulomb Stress Change



$$\Delta\sigma_c = \Delta\tau_r - \mu(\Delta\sigma_n - \Delta p)$$

Coulomb Stress Failure

Friction coef.

$\Delta\sigma_c = \Delta\tau_r - \mu'(\Delta\sigma_n)$

Pore Fluid Pressure

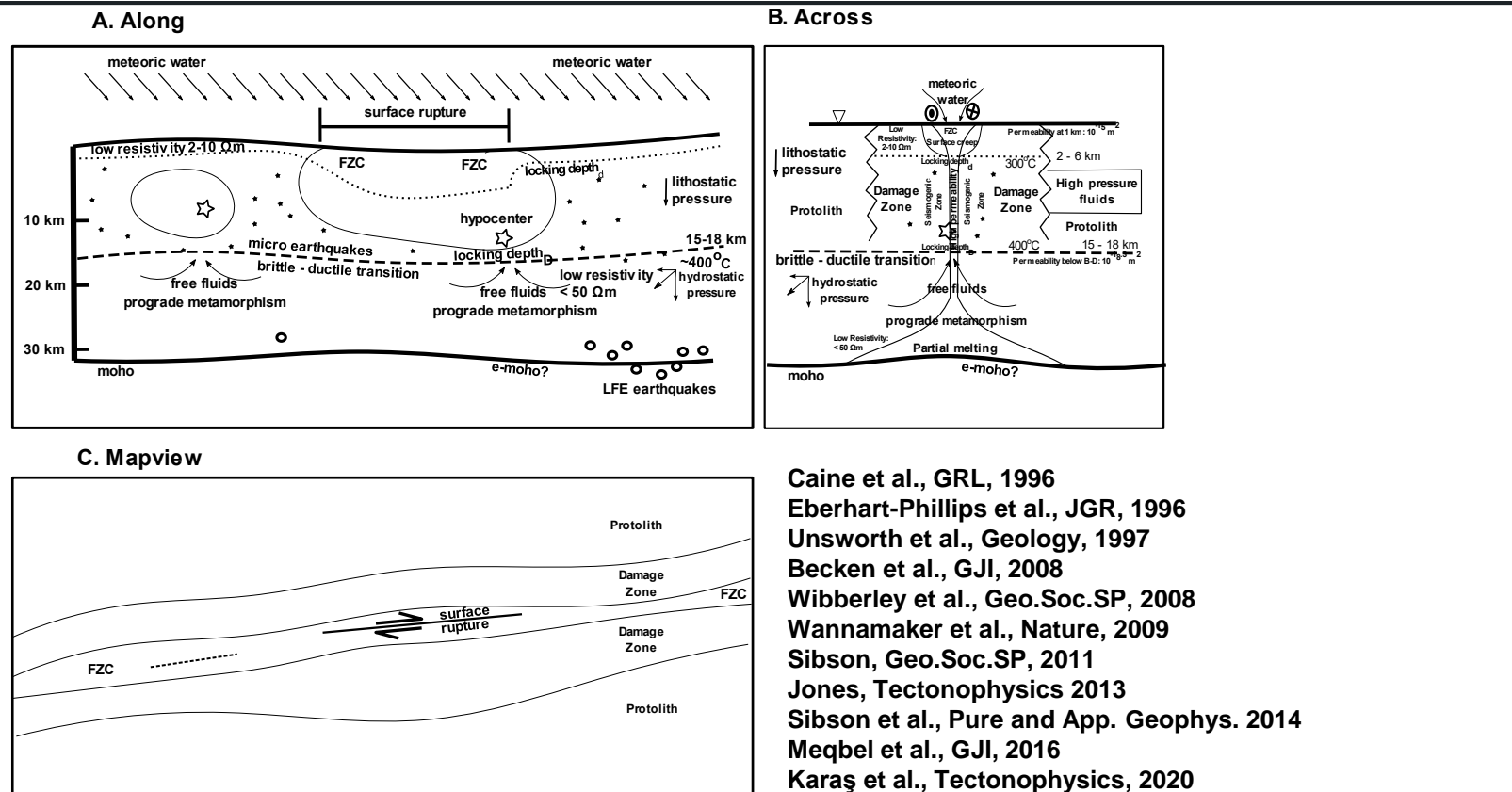
Effect of fluids

Change in Shear Stress

Change in Normal Stress

Scholtz, The Mechanics of Eq. and Faults, 2002
Beeler et al., JGR, 2000

Fault Zone Architecture – Continental Seismogenic Zone





Pressure build – up/Reduction of shear stress

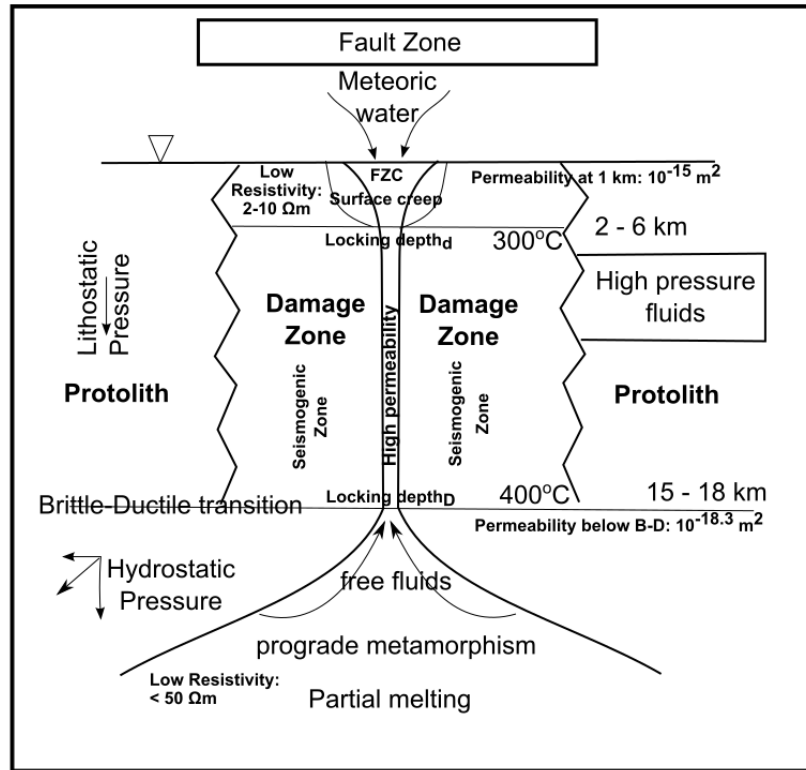
Lubrication – talc/clay

Hydrofracturing and chemical dissolution
Retrograde metamorphism – hydration

Seismic pumping – Fault valve model

Dehydration – free fluids

Prograde metamorphism



Early EM studies on (strike-slip) faults - Theory

30's
The telluric method



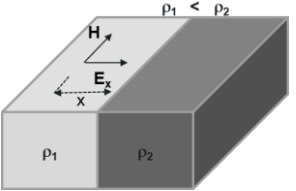
Schelkunoff,
Bell systems, 1938

The Impedance Concept and Its Application to Problems of
Reflection, Refraction, Shielding and Power Absorption

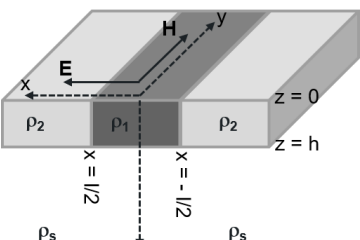
By S. A. SCHELKUNOFF

This paper calls attention to the practical value of a more extensive use of the impedance concept. It shows how the impedance underlies the theory in what otherwise appear diverse physical phenomena. Although an attempt has been made to trace the history of the concept of "impedance" and many interesting early suggestions have been found reference to these lies beyond the scope of this paper. Still, it is felt that this is the first time the word "impedance," but the concept has been developed gradually as circumstances demanded through the efforts of countless workers.

The main body of the paper is divided into three parts: Part I, dealing with the exposition of the impedance idea as applied to different types of physical phenomena; Part II, in which the general formulae are deduced for reflection and transmission coefficients; Part III, presenting a number of applications illustrating the practical utility of the foregoing manner of thought.



d'Erceville and Kunetz,
Effect of a fault on the
Earth's natural EM field,
1962



Weaver,
Discussion,
1963

Rikitake, 1948, Tikhonov, 1950
Cagniard, Geophysics, 1953

BASIC THEORY OF THE MAGNETO-TELLURIC METHOD
OF GEOPHYSICAL PROSPECTING*†

LOUIS CAGNIARD

ABSTRACT

From Ampere's Law (for a homogeneous earth) and from Maxwell's equations using the concept of Hertzian wave propagation, the basic equations are obtained for the propagation of the electric and magnetic fields in the presence of telluric currents in the earth. The ratio of these horizontal components, together with their relative phases, is diagnostic of the structure and properties of the earth. The apparent resistivities and phase differences of the currents are similarly diagnostic.

From the above, magnetotelluric sounding is represented by curves of the apparent resistivity and the phase difference at a given station plotted as functions of the period of the various telluric currents. These curves are compared with the corresponding curves obtained with the two- and three-layer problems.

For the two-layer problem, the geometrical similarity and whose corresponding resistivities differ only by a linear factor, the phase relationships are the same and the apparent resistivities differ by the same factor. This makes it possible to reduce the number of parameters. The use of a "model of simulated" greatly simplifies the representation of a master set of curves, such as is given for use in practice.

In addition to the small advantages offered by the use of telluric currents (no need for current sources), the magnetotelluric method has the great advantage that it is a transient method. This property resolves the effects of individual wells better than do conventional resistivity methods. It seems to be a ideal tool for the initial investigation of large sedimentary basins with potential petroleum reserves.

Wait, Geophysics, 1954

ON THE RELATION BETWEEN TELLURIC CURRENTS
AND THE EARTH'S MAGNETIC FIELD*

JAMES R. WAIT†

ABSTRACT

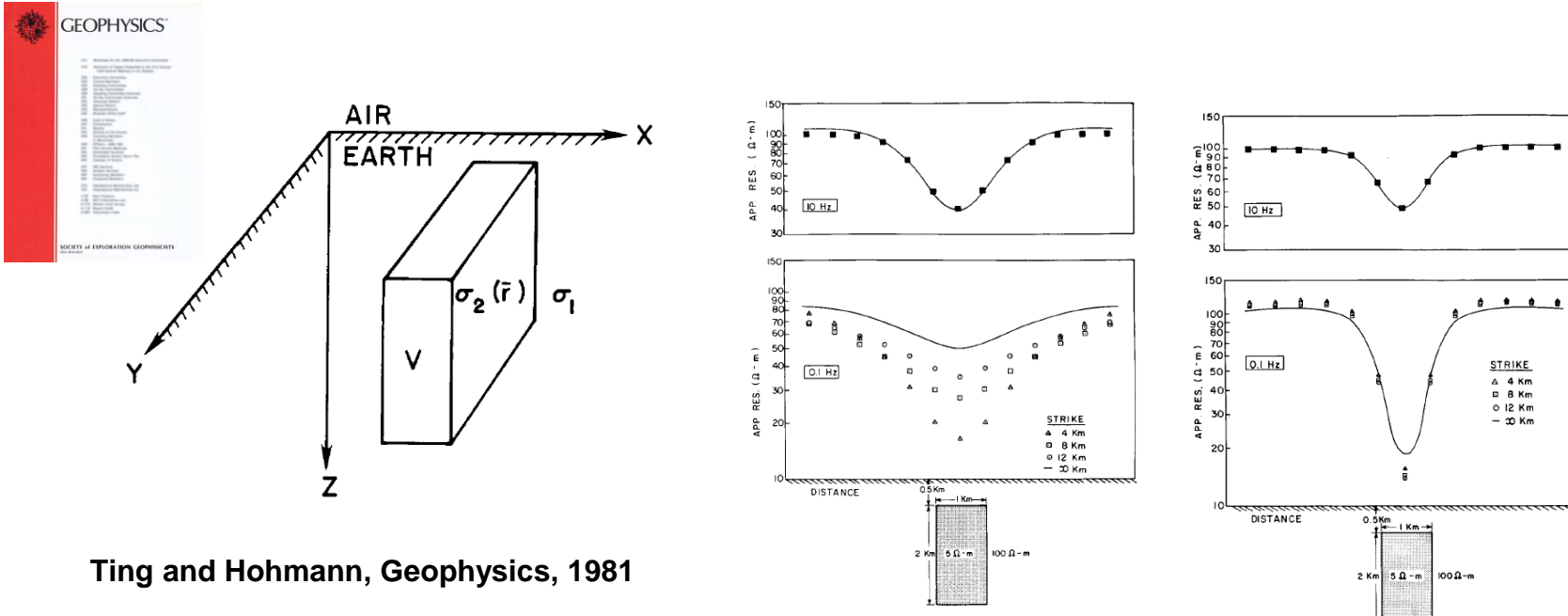
The validity of Cagniard's analysis of the effect of telluric earth currents is reexamined in view of the fact that the components of the electric field and magnetic field tangent to the surface of the ground are only proportional to one another if the fields are sufficiently slowly varying over the surface of the ground. His result is extended to include the effects of a layered ground with both conductivity and susceptibility variations. Finally the corresponding transient problem is solved for a two-layer horizontally stratified earth.

Replies by:
 - d'Erceville and Kunetz (1963)
 - Rankin (1963)

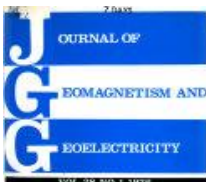
"It seems therefore, that some caution must be exercised in trying to apply the theoretical solutions for the "fault" and "dike" models to a practical situation."

Early EM studies on (strike-slip) faults - Theory

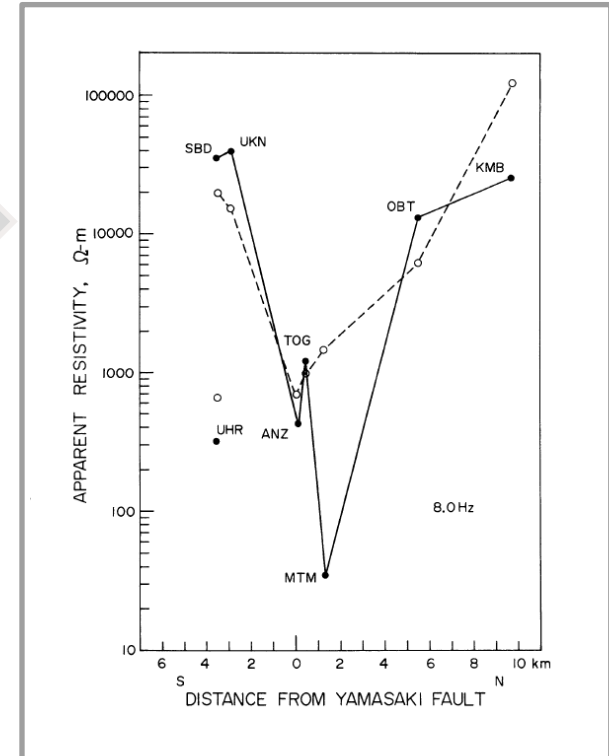
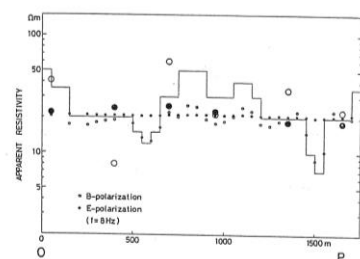
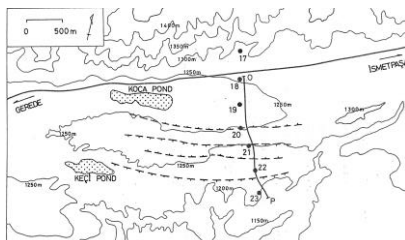
Integral equation modeling of three-dimensional magnetotelluric response



Early EM studies on (strike-slip) faults - Practical



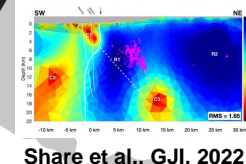
- Reddy et al., JGG, 1976 – SAF
- Lienert et al., JGG 1980 - SAF
- EM Research Group of the Active Fault, JGG, 1982 - Yamasaki F.



Honkura et al., Tech. paper
by Titech and İstanbul Uni., 1986

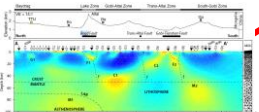
Magnetotelluric studies on major strike-slip fault zones

Tintina F.
GSLake F.
Denalli F.



West F.

Waterberg F.

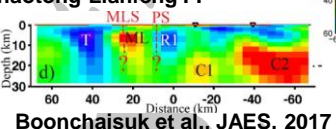


Longlin F.

Derbugan F.
Bogd F.
Altyn Dagh F.

Jiali F.
Kunlun E.
Huya F.

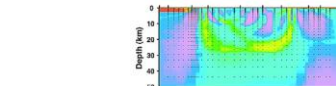
Kachchh M. F.
Tan Shear
Red River F.
Zhaotong-Lianfeng F.



Boonchaisuk et al., JAES, 2017



Wannamaker et al., JGR, 2002



Wannamaker et al., Nature, 2009

Alpine F.

Yoshimura et al., GRL, 2009

Usui et al., 2020

Niigata – Kobe TZ
Atotsugawa F.

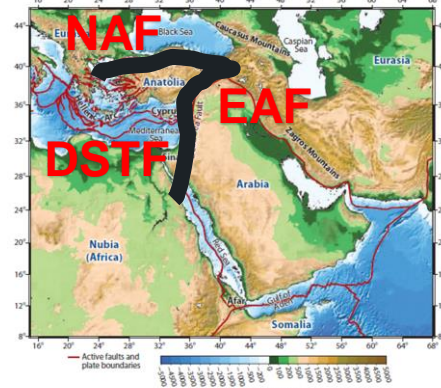
Median Tectonic Line F.

Longlin F.

Xiao et al., JGR, 2017

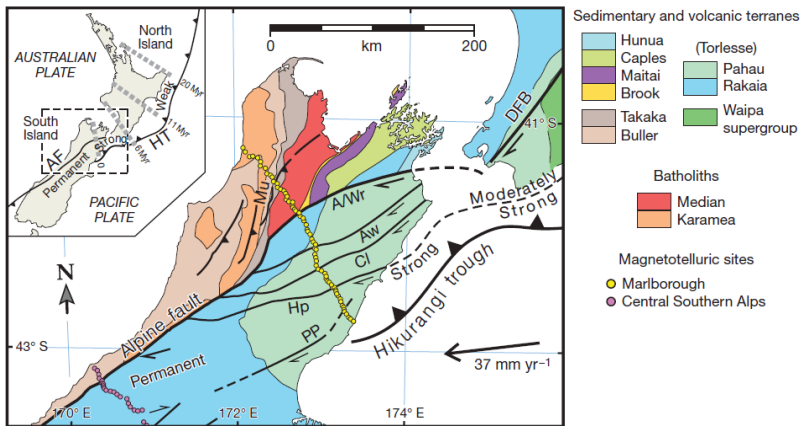
Comeau et al., EPS, 2020

Le Pichon et al., Ann. Rev. Earth and Plan. Sci., 2010

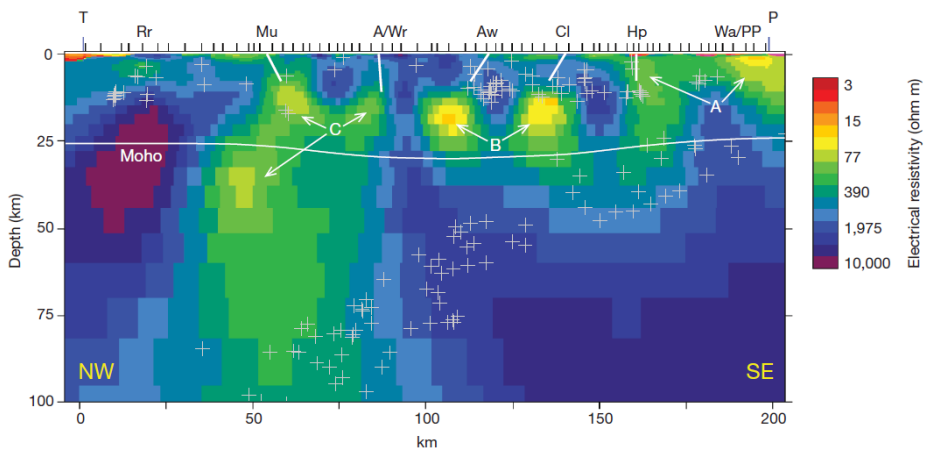


Global examples I:

Alpine Fault, New Zealand (2D)

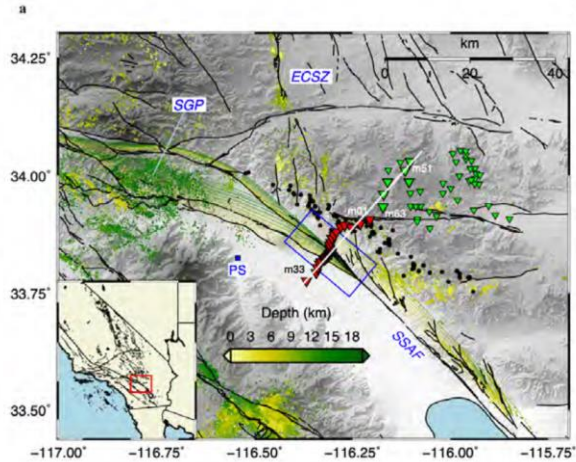


Wannamaker et al., Nature, 2009

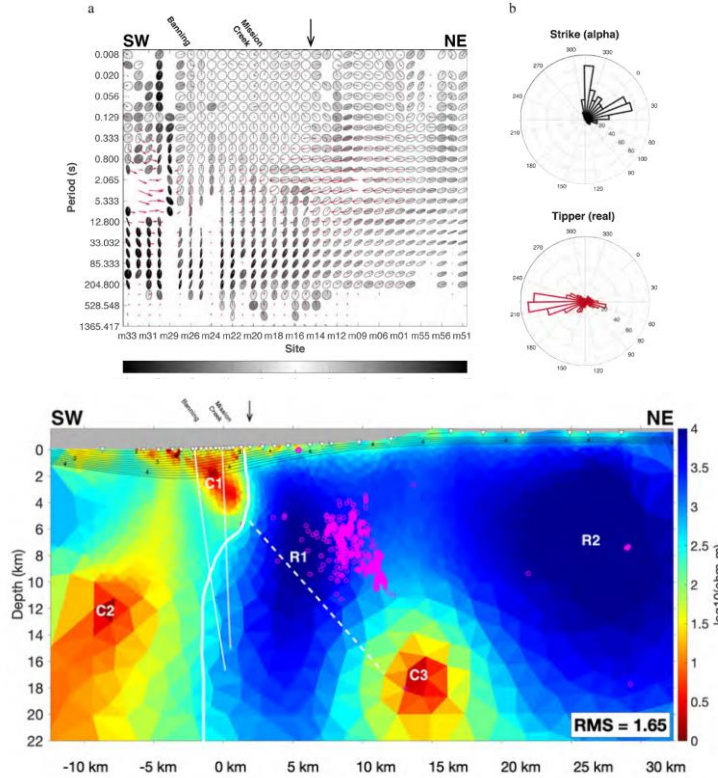


Global examples 2:

Southern San Andreas Fault, California, the USA (2D & 3D)

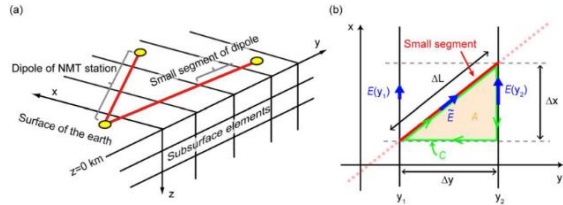
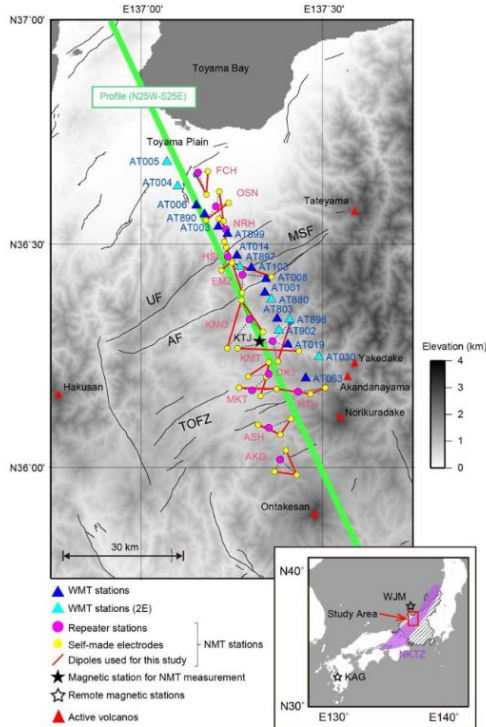


Share et al., GJI, 2022

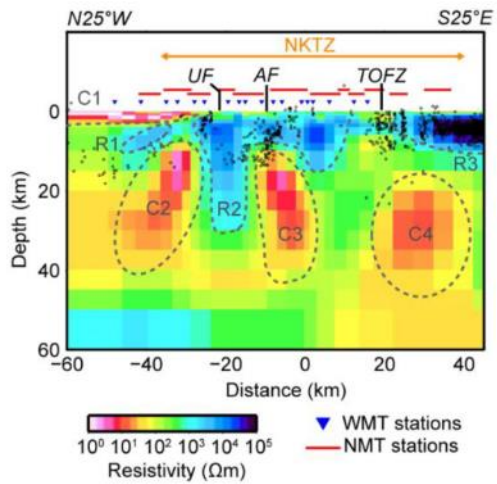


Global examples 3:

Atotsugawa Fault, Central Honshu, Japan (2D)



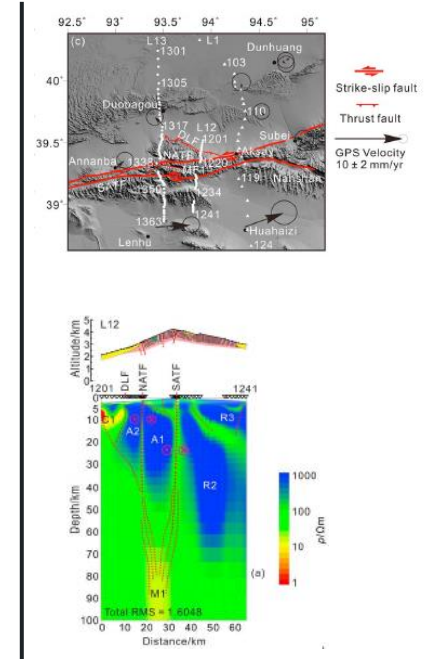
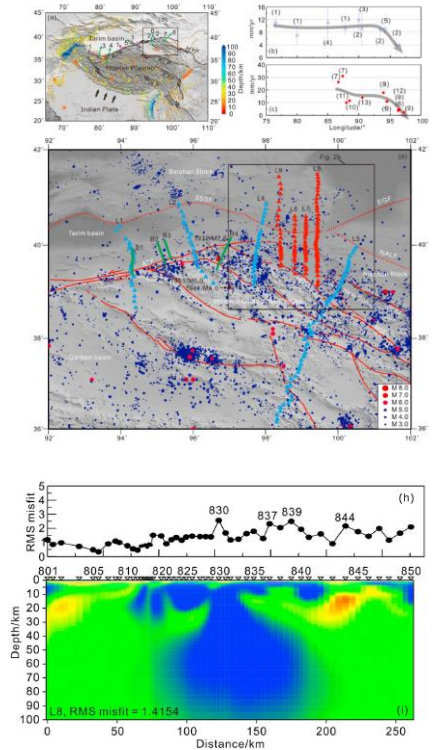
Wideband MT
Wideband MT + Network MT
2D by Ogawa and Uchida, GJI, 1996



Global examples 4:

Altyndagh Fault, NW China

(2D and 3D)

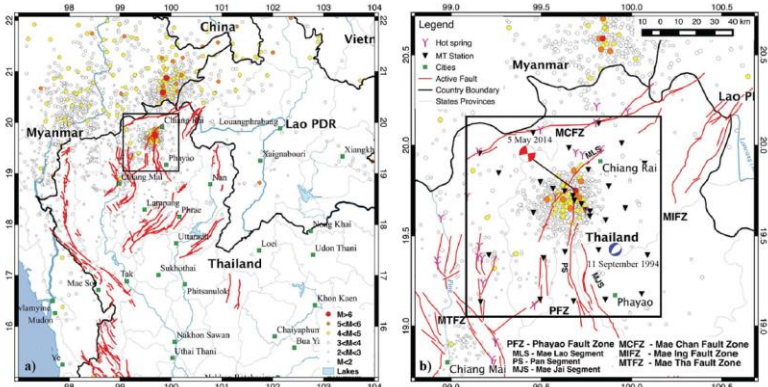


Xiao et al., JGR, 2015

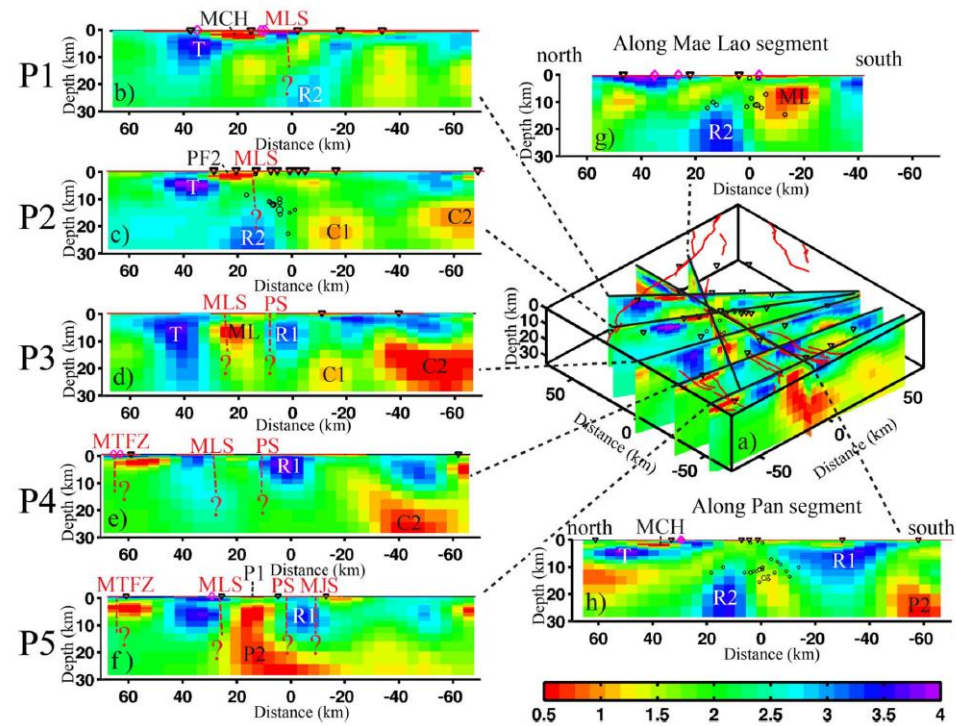
Xiao et al., GRL, 2017

Global examples 5:

Phayao Fault Zone, N.Thailand (3D)

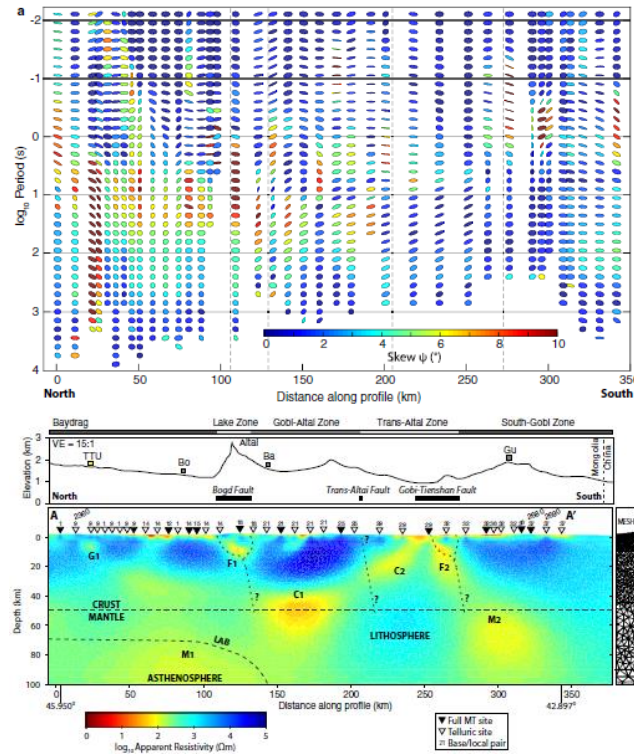
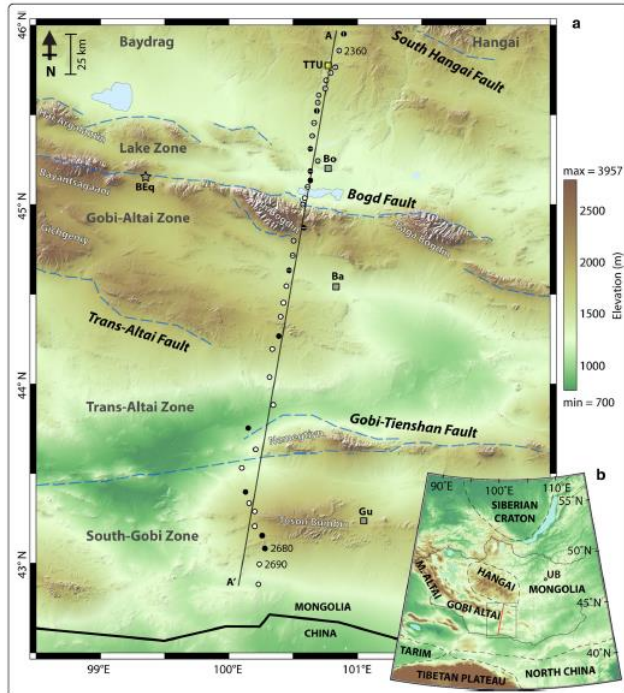


Boonchaisuk et al., JAES, 2017



Global examples 6:

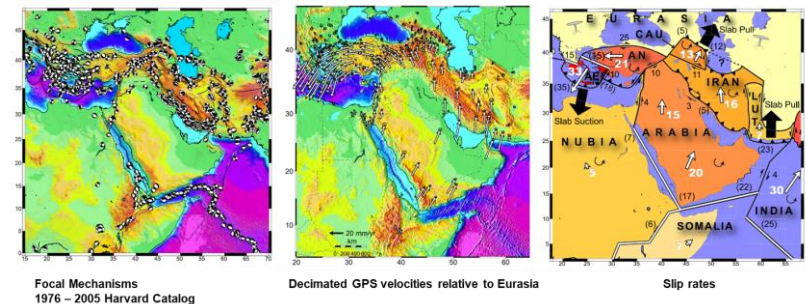
Bogd – Trans Altai – Gobi Tienshan faults, Mongolia (2D)



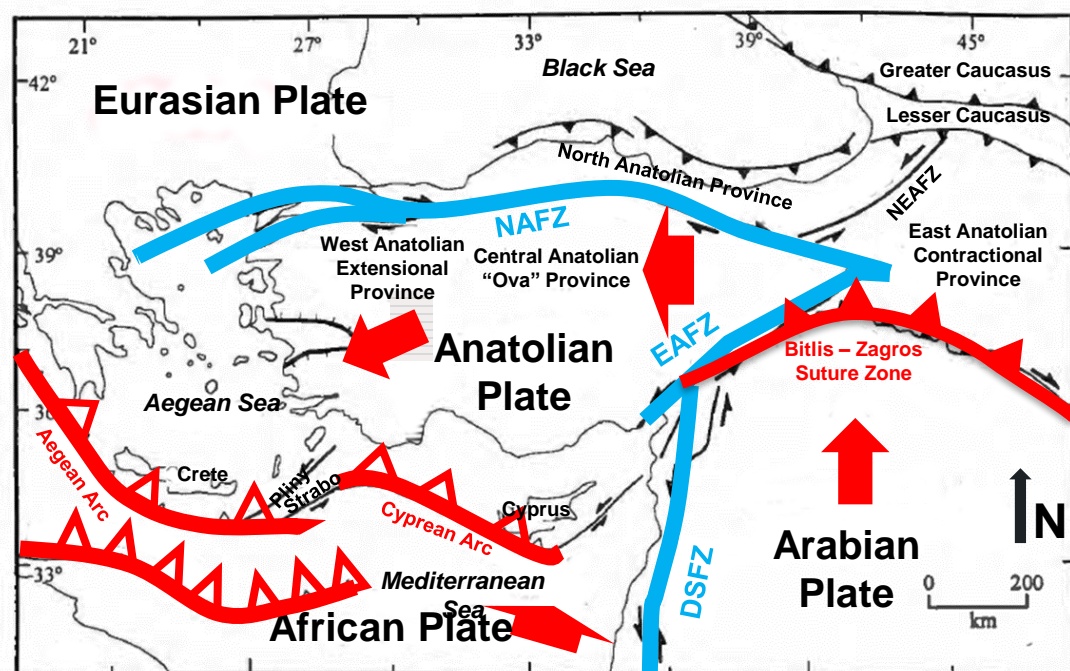
MARE2DEM
39 sites
39 frequencies
TM+TE
300 Ohmm initial model

Eastern Mediterranean - Tectonics

1. Arabian Promontory
2. East Anatolian Contractual Province
3. North Anatolian Province (Pontides)
4. Central Anatolian "Ova" Province
5. West Anatolian Extensional Province



Reilinger et al., JGR, 2006

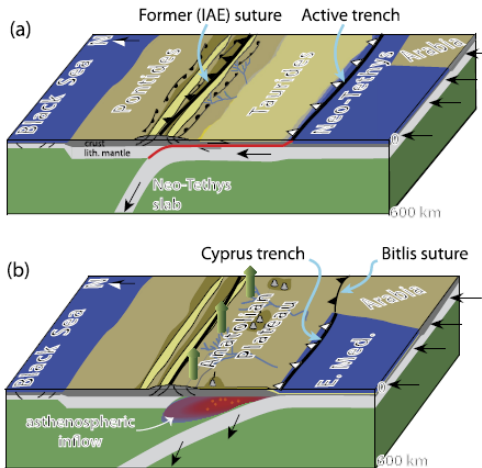


Bozkurt, GeoActa, 2001

Sengör et al., SEPM Society for Sedimentary Geology, 1985

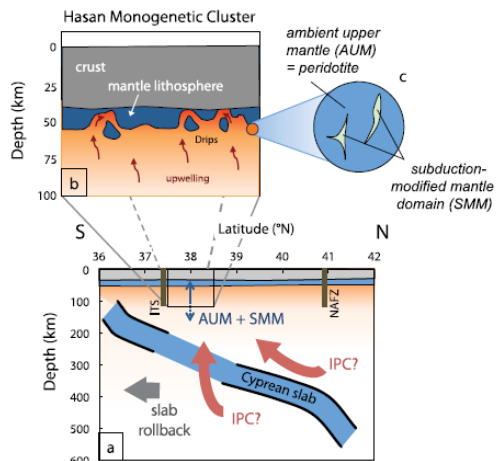
Tectonic models

Delamination



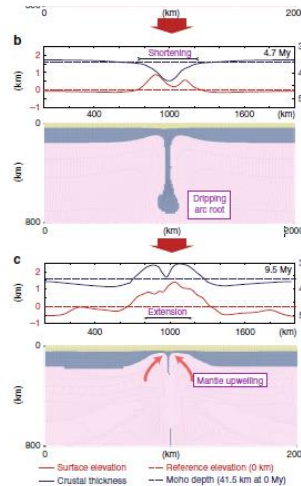
Govers and Fichtner, EPSL, 2016;
 Bartol and Govers, Tectonophysics, 2014

Delamination and drip

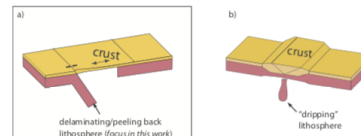


Reid et al., G-cubed, 2017

Drip tectonics



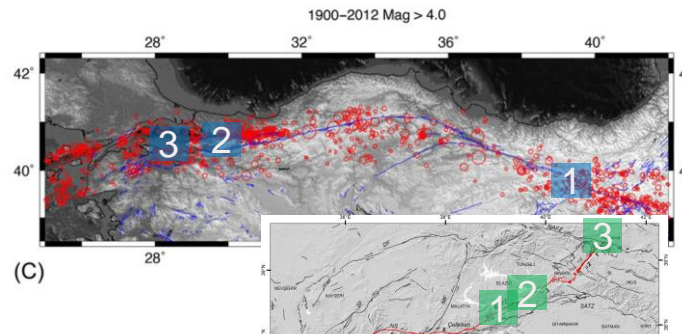
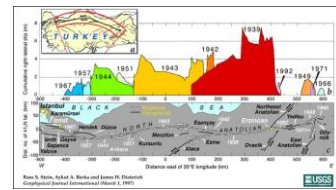
Göğüş et al., Nature Comm., 2018



Göğüş and Ueda, JDyn, 2018

A collage of transform faults:

Dead Sea Transform – East and North Anatolian Faults



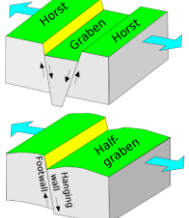
(C)

Karlıova
Triple Junction

Maraş
Triple Junction

Hatay
Triple
Junction

Ben-Avraham et al., 2008
Division of DSTF
At 33°10'N



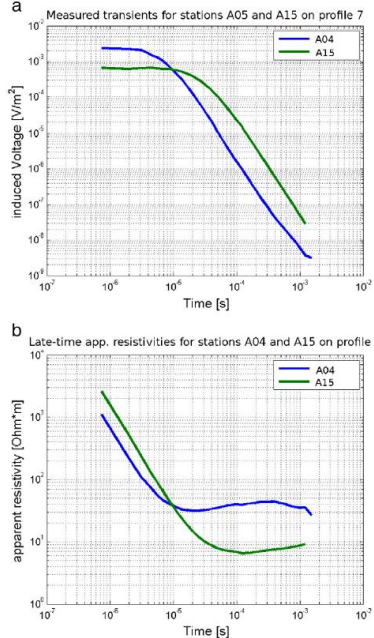
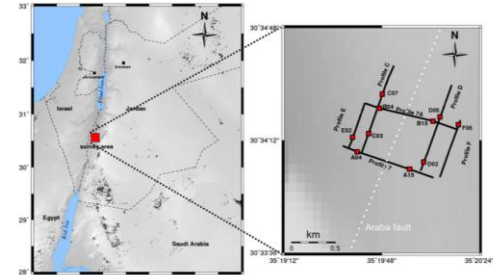
NAF: ~ 1500 km
Dextral - 85 km
Westward progression of eqs.
7.4 İzmit eq 1999
7.2 Düzce eq 1999

EAF: ~ 500 km
Sinistral - 22 km
6.3 Adana-Ceyhan eq. 1998
6.4 Bingöl eq. 2004
6.7 Elazığ eq. 2020
7.7 Gaziantep eq. 2023
7.6 Kahramanmaraş eq. 2023

DSTF: ~ 1000 km
North and south parts
Sinistral – 100 - 107 km
7.3 Aqaba eq. 1995

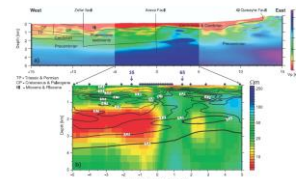
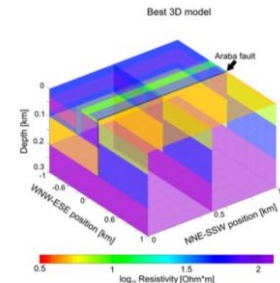
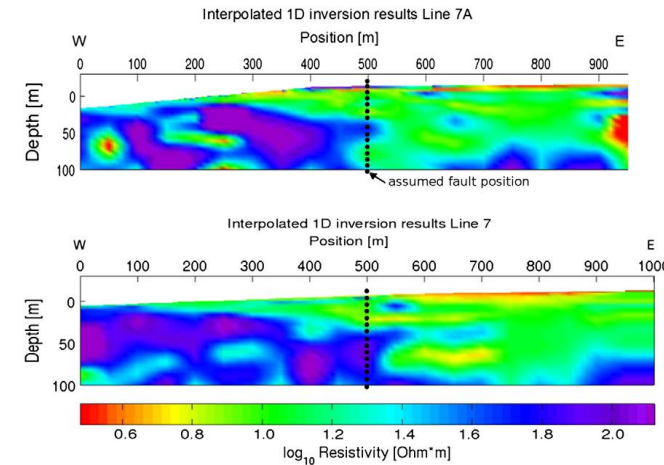
Dead Sea Transform Fault (DSTF) (1D)

Avara/Araba Fault - Short-Offset Transient Electromagnetics (SHOTEM)



- 72 inloop soundings
- 6 profiles in varying length and orientations
- 50 m site separation
- 1D Occam – Marquardt inversions
- 2D and 3D fwd models

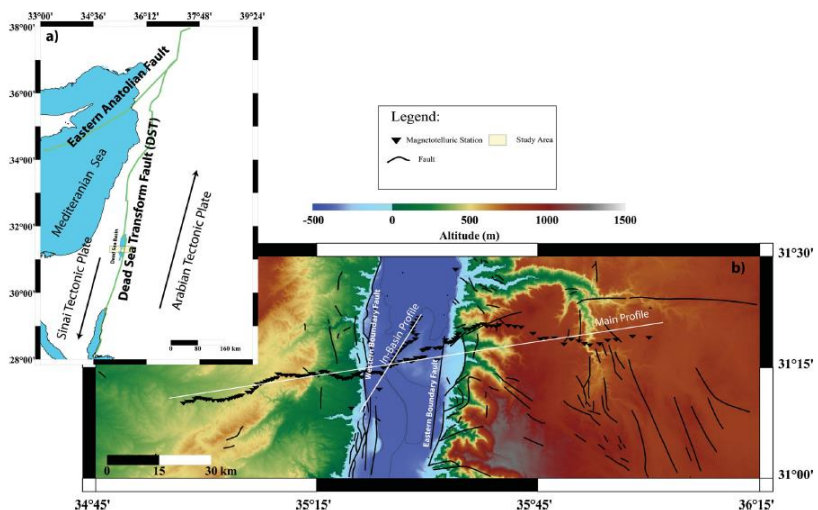
Rödder and Tezkan, Journ. App. Geophys., (2013)



Ritter et al., GRL, 2003

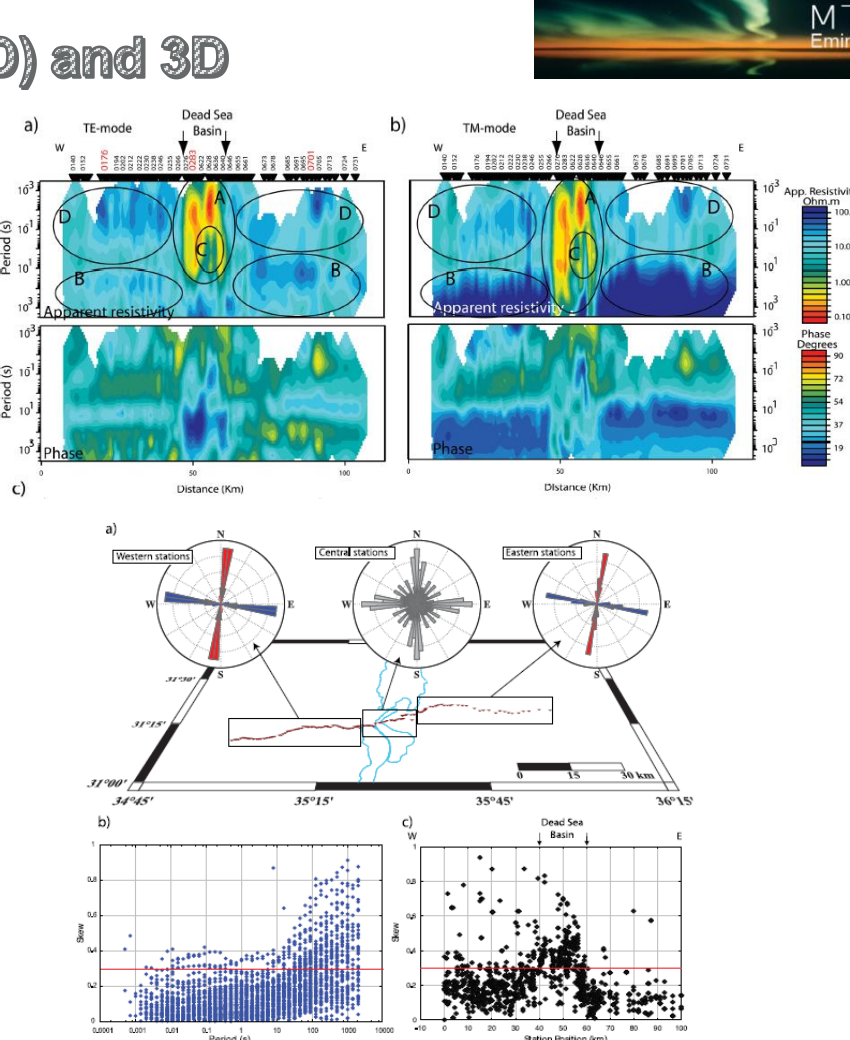
Dead Sea Transform Fault (DSTF) (2D) and 3D

Dead Sea Basin - DESIRE project



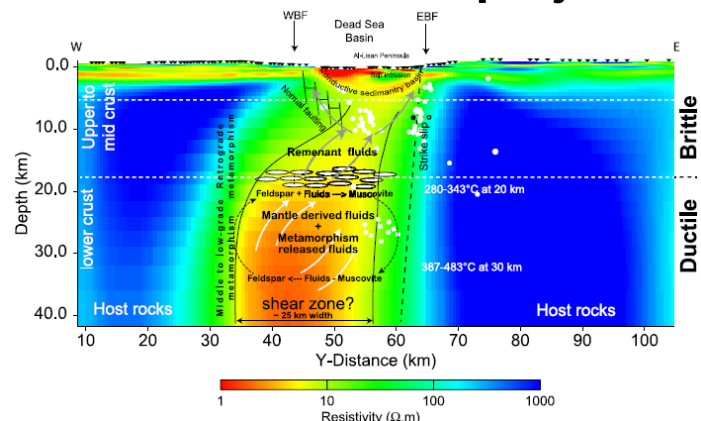
153 observations (94 main p. + 59 auxiliary p.)
 3 days recording at each site
 2 teams and 30 instruments
 Main profile length: 110 km
 2nd profile length: 20 km
 Site separation: 0.5 – 2 km

Meqbel et al., GJI, 2013



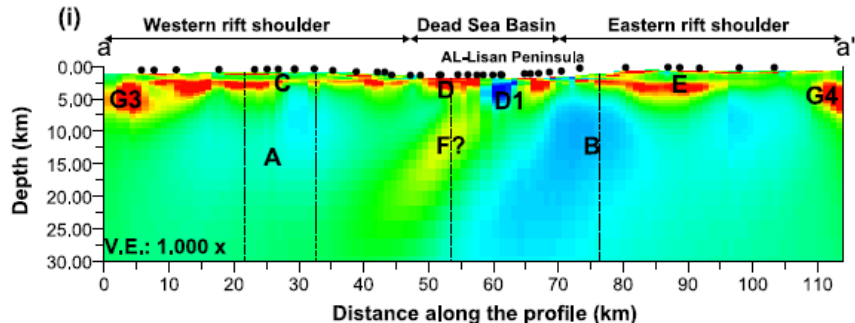
Dead Sea Basin - DESIRE project

(2D)



Meqbel et al., GJI, 2013

(3D)



Meqbel et al., GJI, 2016

Remote reference
N12 E strike angle

2D

Rodi and Mackie (2001) - WinGLink - FD - NLCG

248 x 127 cells

1000 % error floor for TE Rho_a (to deal with static shifts)5 % error floor for TM rho_a

0.6 error floor for both phase

0.03 error floor for Hz

RMS: 12.5 to 1.81 in 2000 iterations

3D

ModEM

NLCG – FD

Nested mesh modeling

1st 70 x 70 (coarse grid)

100 layers including topography and air

20 periods

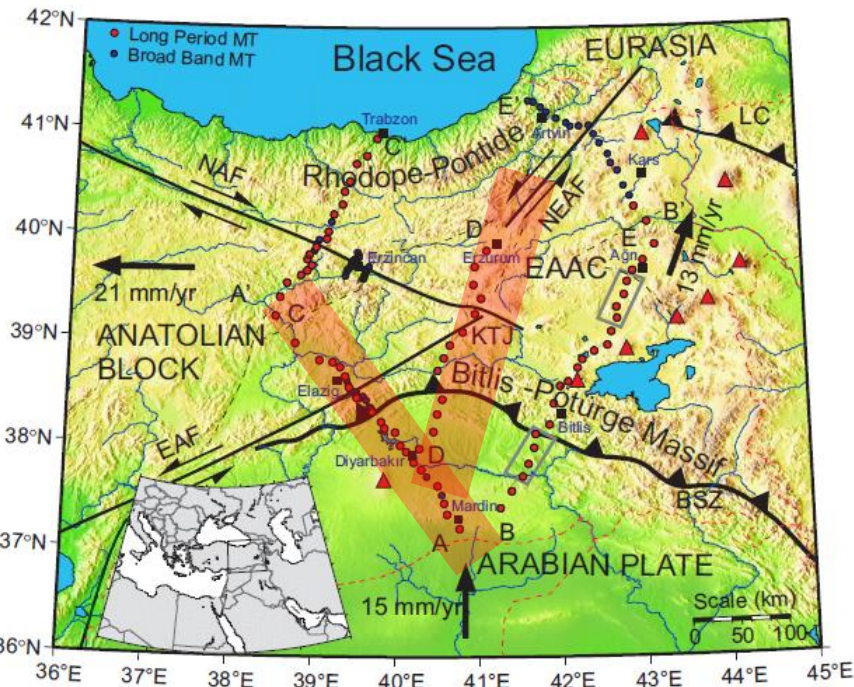
Error floor 5 %



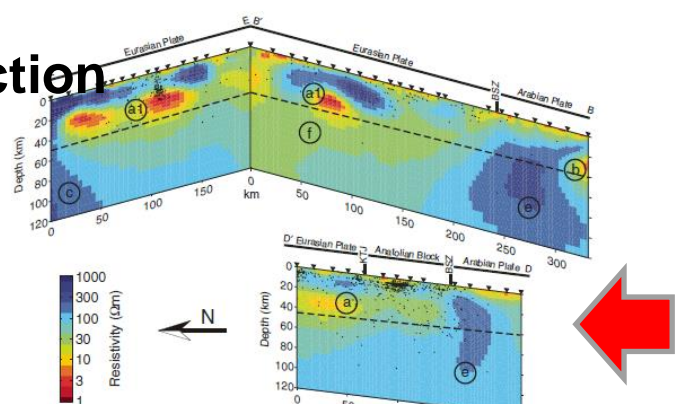
East Anatolian Fault (2D)

Elazığ segment and Karlıova Triple Junction

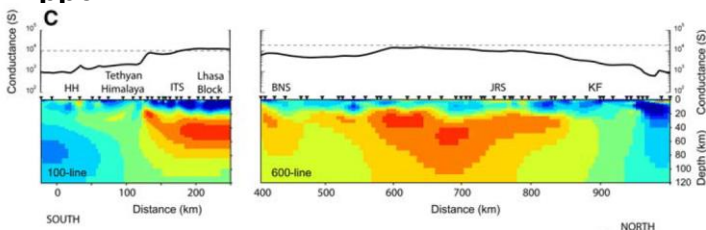
Long period + Wideband



Türkoğlu et al., Geology, 2008

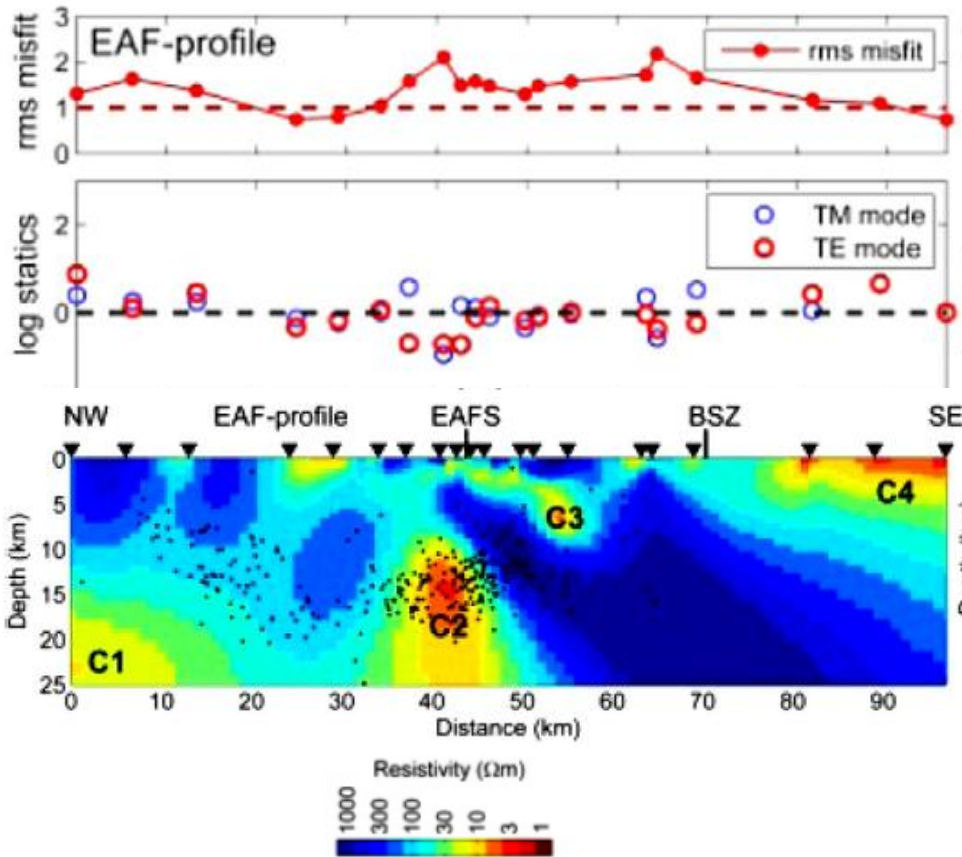
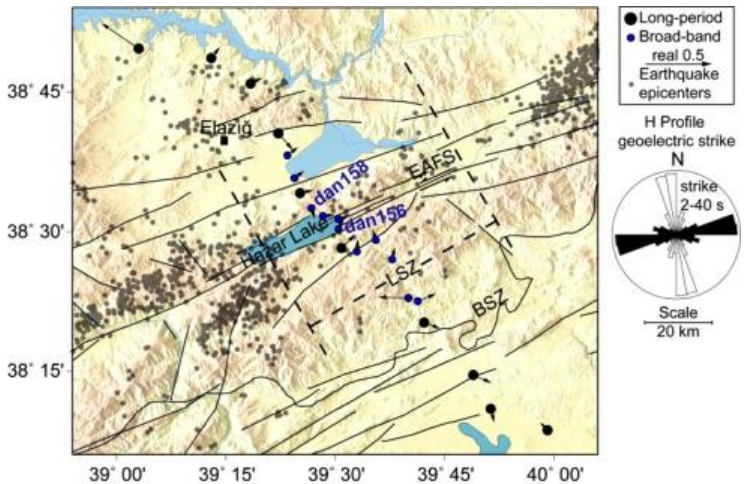
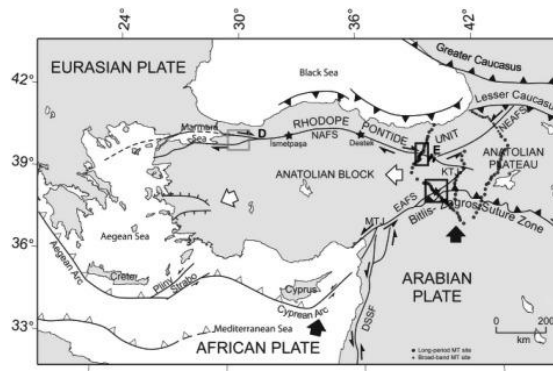


Rodi and Mackie (2001) – NLCG – FD
TE + TM + Tipper



Unsworth., Surveys in Geophysics, 2010

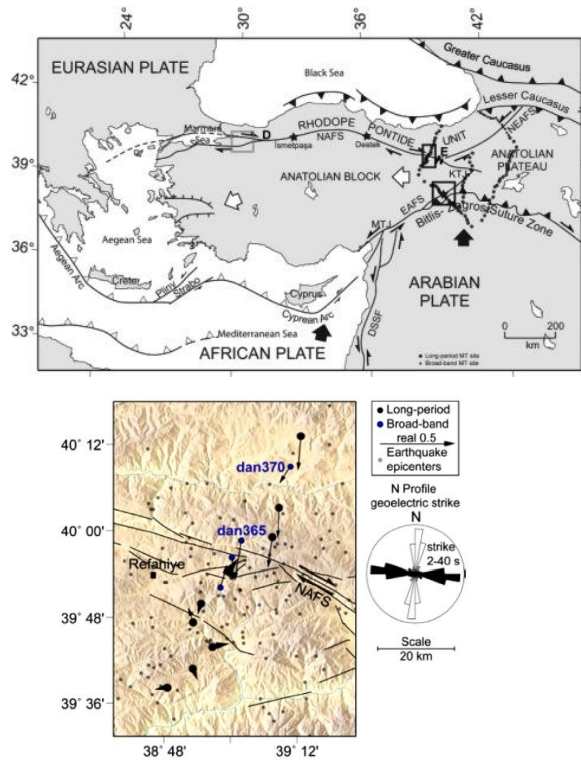
East Anatolian Fault (2D)



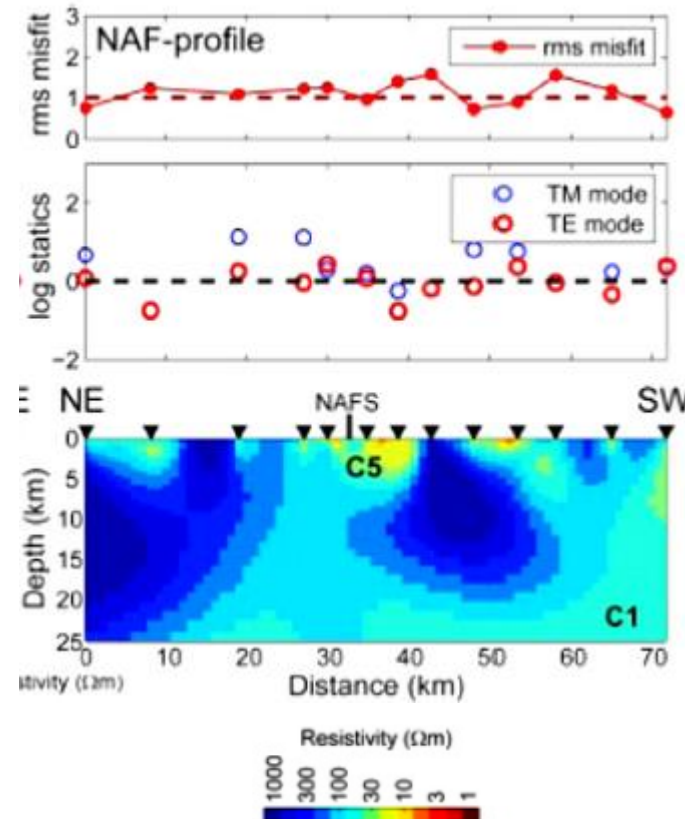
Türkoğlu et al., PEPI, 2015

North Anatolian Fault (East) (2D)

Erzincan segment

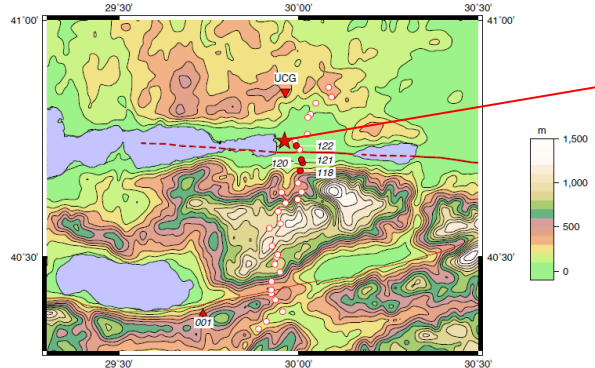


Türkoğlu et al., PEPI, 2015

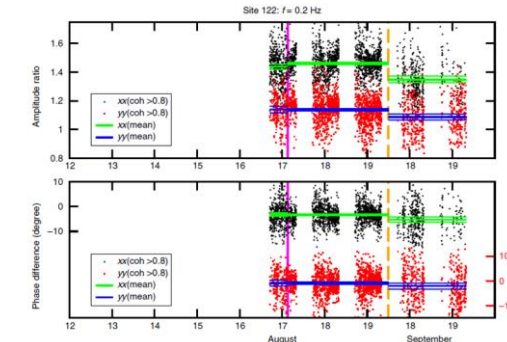
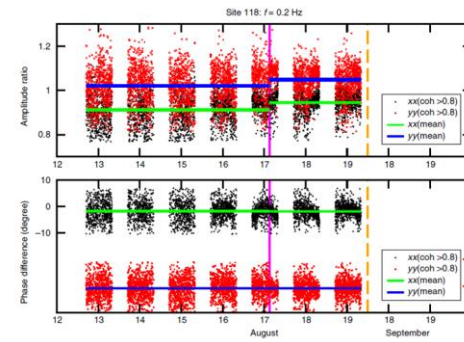
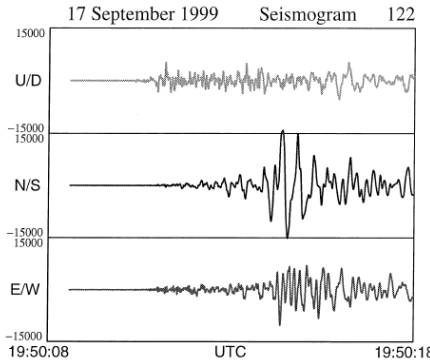
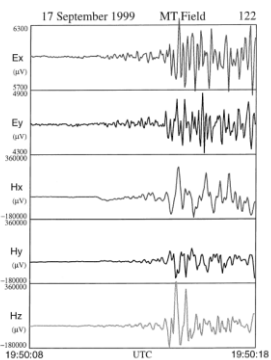


North Anatolian Fault (West)

1999 Izmit Earthquake data

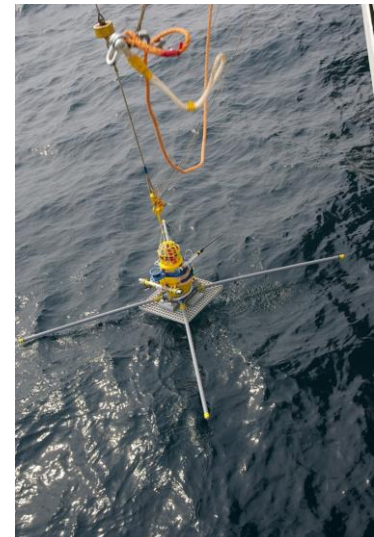
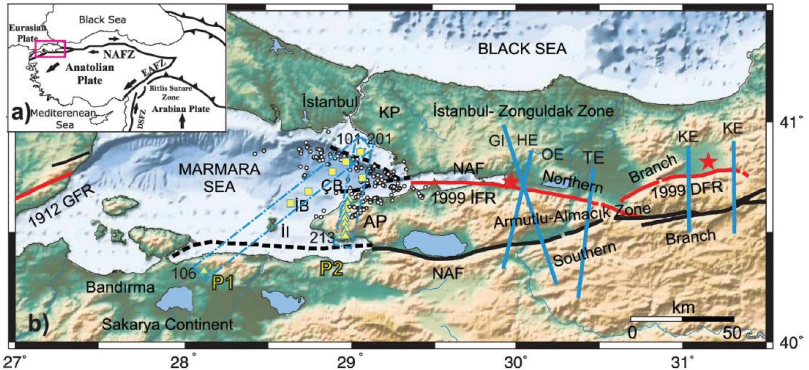


**17 August 1999 Izmit Earthquake
M: 7.4**



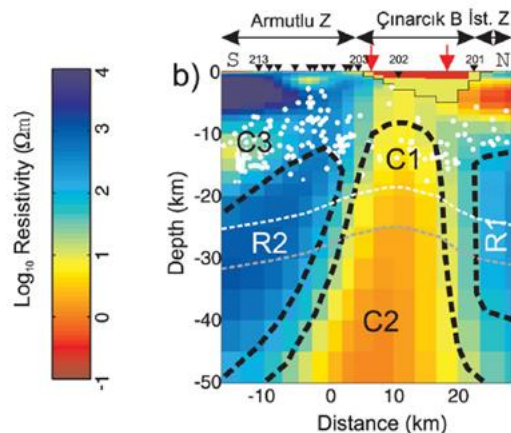
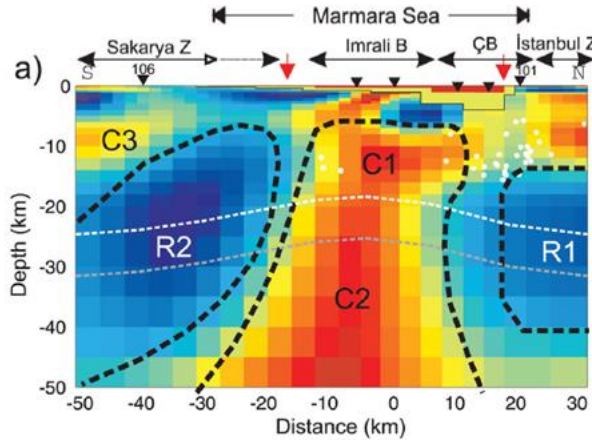
North Anatolian Fault (West) (2D)

Marmara Sea – OBEM

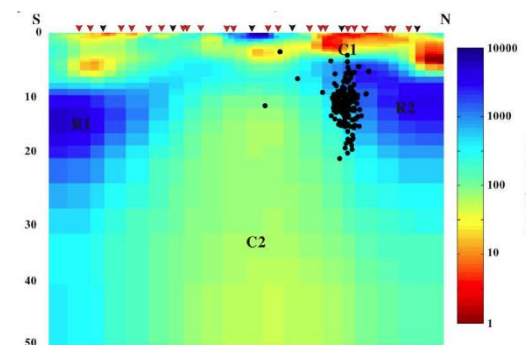
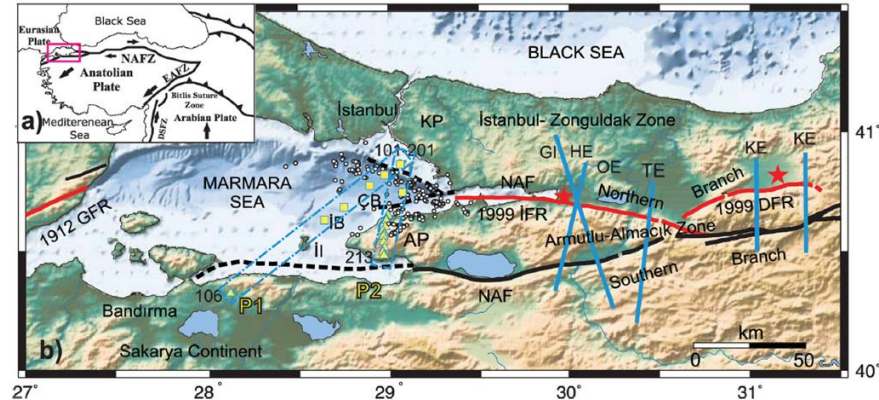


North Anatolian Fault (West) (2D)

Marmara Sea – OBEM

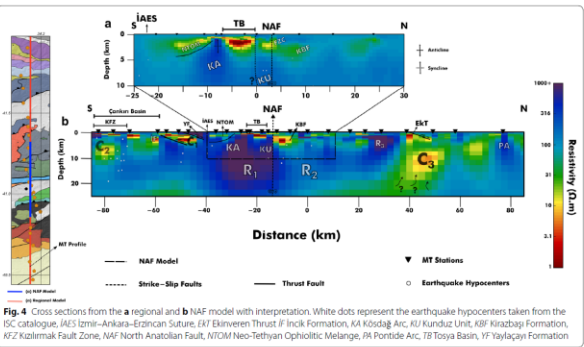
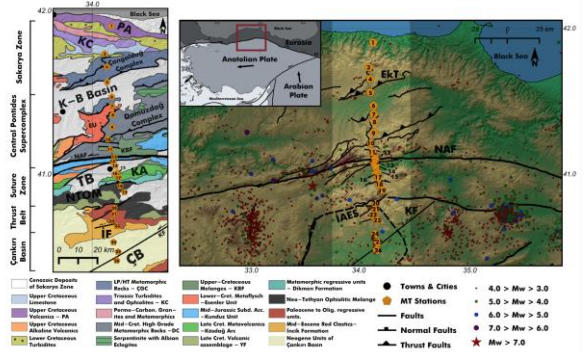


Kaya et al., GJI, 2013

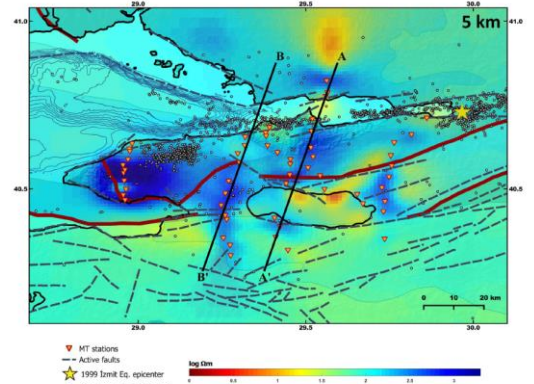
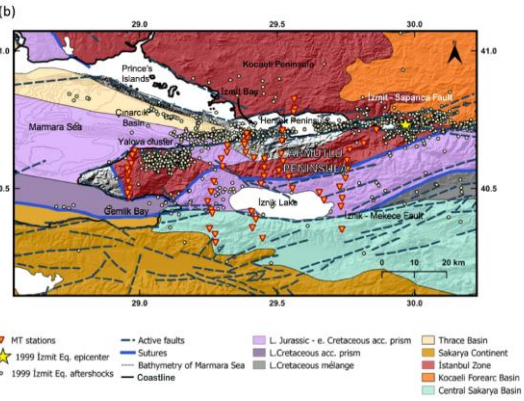


North Anatolian Fault (3D)

Near Tosya



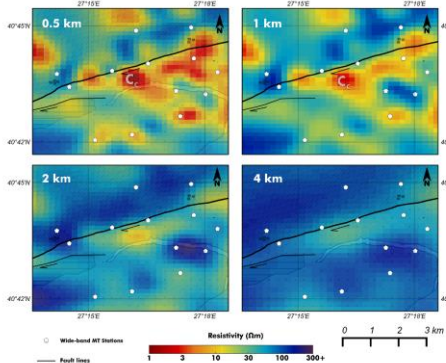
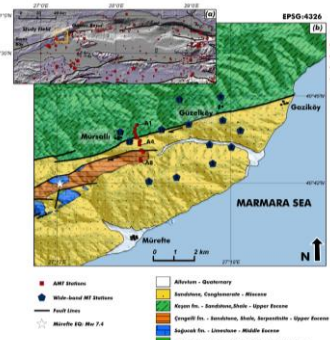
West of İzmit



Özaydın et al., EPS, 2018

Karaş et al., Tectonophysics, 2020

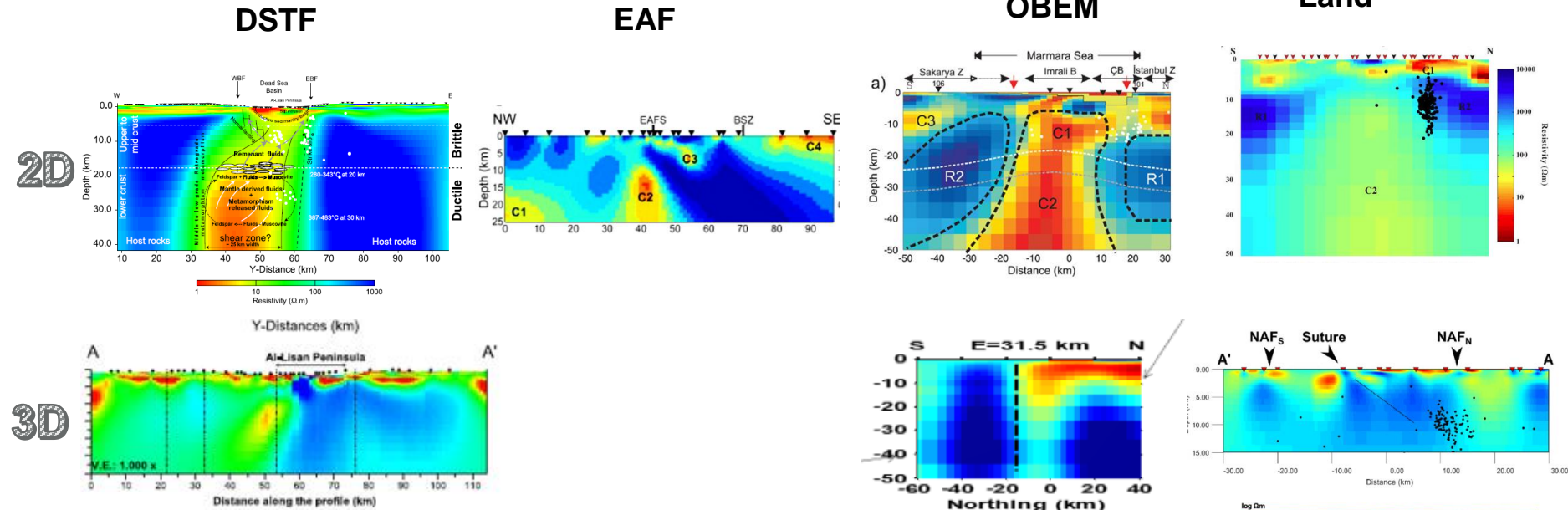
Ganos



Karaş et al., EPS, 2017

Conclusion 1 – Eastern Mediterranean

2D vs. 3D



Meqbel et al., GJI, 2013; 2016

Türkoğlu et al., PEPI, 2015;
Geology, 2008

Kaya et al., GJI, 2013;
Karaş et al., Tectonophysics, 2020;
Tank et al., PEPI, 2005

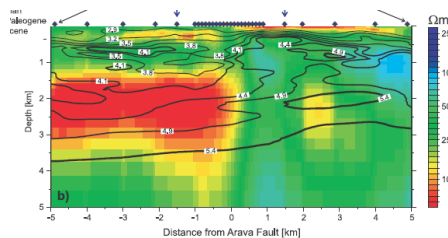
Conclusion 2

Shallow structure
Fault Zone Conductors - Comparison

DSTF : No FZC
NAF : Surface – 0.7 km (locked)
SAF : Surface – 3 km (locked)
Surface – 6 km (creeping)

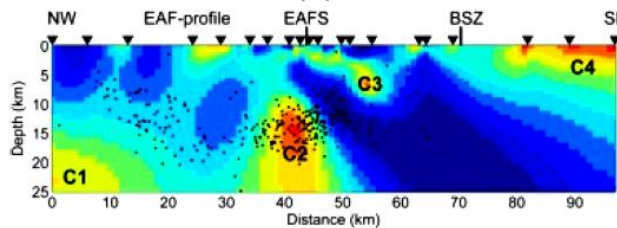


DSTF

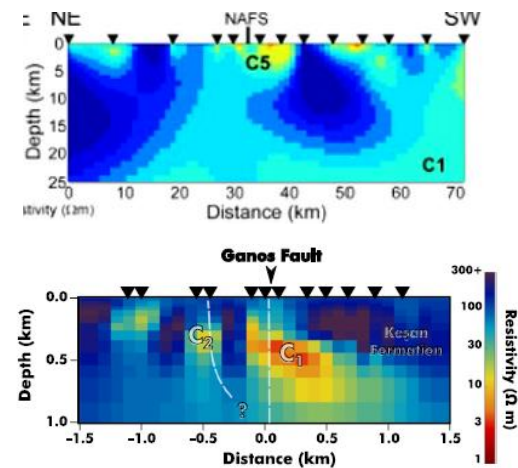


Ritter et al., GRL, 2003

EAF



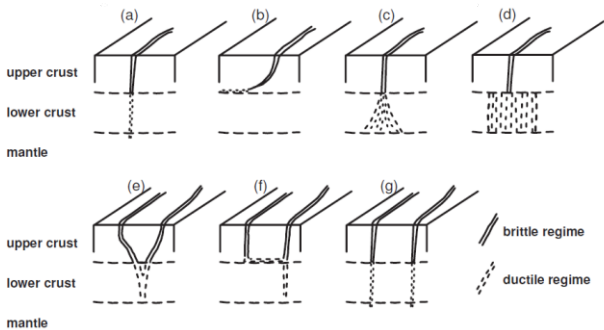
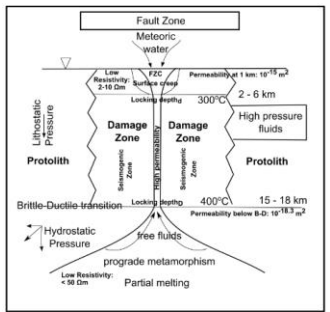
Türkoğlu, PEPI, 2015



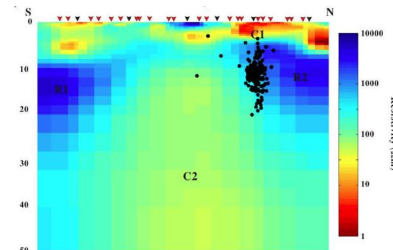
Karaş et al., EPS, 2017

Conclusion 3

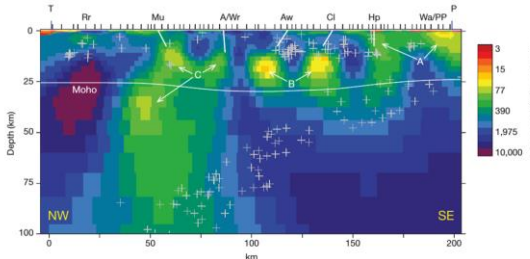
Deep structure Comparison



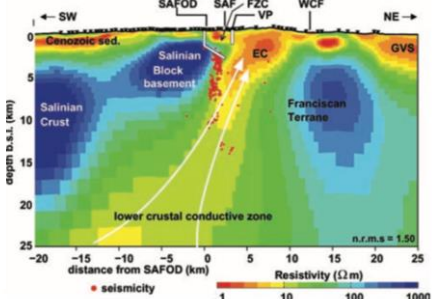
Ritter et al., Spec. Pub, 2005



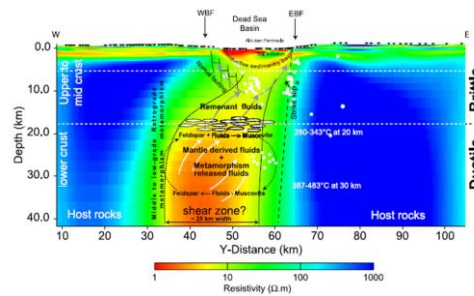
NAF – Tank et al., 2005



Alpine Fault – Wannamaker et al., 2009



SAF - Becken et al., 2008

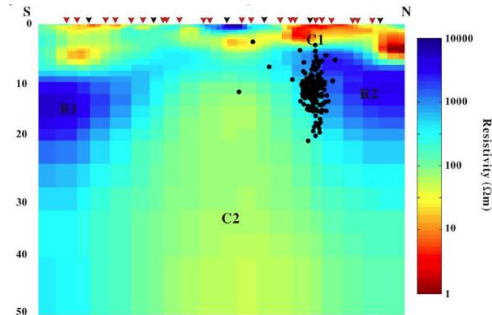
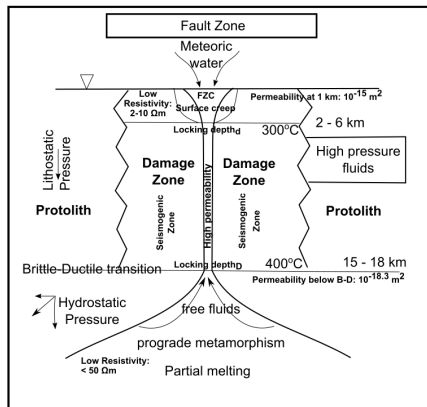


Meqbel et al., 2013; 2016



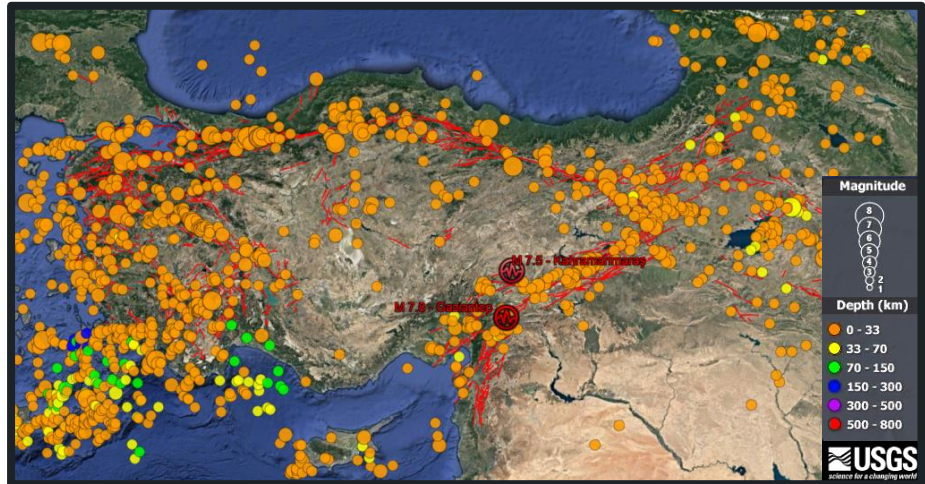
Conclusion

- Fluids may have an essential role in the earthquake generation
- Fluid presence at a fault zone can be detected by using EM methods almost at all depths
- Narrative review based on electrical structure of transform faults
- Historical and global perspective to the topic
- Three major transform faults of the eastern Mediterranean

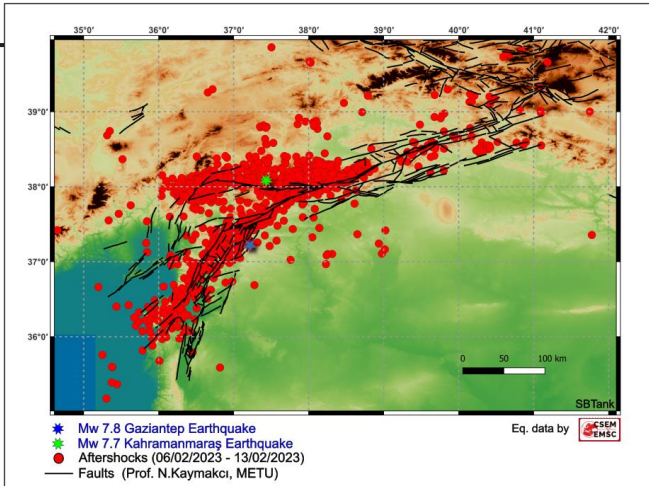




Invitation - Call for projects



Earthquakes 1900 – 2023 (Source: USGS)



Aftershocks 06/02 – 13/02/2023 (Source: EMSC)

- Example for stress transfer
- Faults – Fluids
- Active seismicity
- Tectonics - triple junction(s)
- Multi - disciplinary approach

S.Bülent Tank: bulent.tank@boun.edu.tr
B.U. Kandilli Obs. E.R.I., Geophysics Dept.
34684, Çengelköy, İstanbul, Turkey